Composites Science and Technology 242 (2023) 110205

Contents lists available at ScienceDirect

Composites Science and Technology

journal homepage: www.elsevier.com/locate/compscitech

Influence of printing parameters and short carbon fibre reinforcement on fatigue behaviour, dimensional accuracy and macrogeometrical deviations of polylactic acid in material extrusion

Carolina Bermudo Gamboa, Sergio Martín-Béjar *, Javier Trujillo Vilches, Lorenzo Sevilla Hurtado

Department of Civil, Materials and Manufacturing Engineering, EII, University of Malaga, 29071, Malaga, Spain

ARTICLE INFO

Keywords:
Additive manufacturing
Polylactic acid
Short carbon fibres
Material extrusion
Printing parameters
Fatigue behaviour
Dimensional accuracy

ABSTRACT

This paper evaluates the potential of short carbon fibres as a reinforcement material in order to improve the fatigue resistance of PLA. The fatigue behaviour has been analysed through rotational bending fatigue tests. The influence of printing parameters, such as layer thickness, printing temperature and printing speed, on the mechanical behaviour, dimensional accuracy and macrogeometrical deviations of printed parts have also been analysed as they can too interfere with the mechanical behaviour of the parts. The results show that there is no improvement on the mechanical behaviour of the printed parts with the incorporation of short carbon fibres. On the contrary, the fatigue behaviour worsens due to the poor adhesion between the short carbon fibres and the PLA matrix. Fatigue life is reduced by 6% compared to PLA. Focusing only on the printing parameters, it is shown that at the highest temperature allowed, the fatigue behaviour improves a 12%. The Printing speed is the least influential variable, with the layer thickness having the greatest influence, increasing fatigue life by 15% comparing 0.1 mm and 0.3 mm. Therefore, the best combination would be to print with the highest temperature and the highest layer thickness, for this case study. Finally, a parametric relationship is presented in order to relate the layer thickness with the fatigue behaviour.

1. Introduction

Fused Filament Fabrication (FFF) is one of the additive manufacturing (AM) technologies most widely used [1–3]. FF involves the deposition of extruded thermoplastic material in a layer-by-layer manner to create a three-dimensional object [4]. One of the major advantages of FFF is its versatility in terms of material selection [5]. Another advantage of FFF is its relatively low cost and ease of use compared to other Additive Manufacturing (AM) processes such as selective laser sintering (SLS) or Stereolithography (SLA). On the other hand, one of the main problems when working with FFF is the large number of variables to control [6,7]. It is well known that these parameters influence the final printed parts geometrically, dimensionally and mechanically. However, the large number of parameters and the interaction between them present a difficulty when deciding on their optimal selection [8,9]. Layer height, printing speed, nozzle diameter, and printing temperature are among the most important parameters that affect the mechanical properties of printed parts [10].

One of the most widely processed materials is polylactic acid (PLA) along with acrylonitrile butadiene (ABS). The advantage of PLA over ABS is that it is a biodegradable and renewable thermoplastic material derived from renewable sources such as corn starch or sugarcane. It is easy to use, produces less emissions during printing, and has low toxicity, making it a popular choice for applications in medical [6], aeronautical [11] and electronics industries among others [12]. Additionally, PLA has a much better printability than ABS.

Knowing that PLA has limited mechanical properties, researchers have been working on the implementation of different reinforcement materials to address these mechanical limitations. Short carbon fibres are known to enhance the mechanical properties of PLA, such as stiffness and strength, due to their high aspect ratio and high tensile modulus. The fibres can improve the material fatigue resistance, making it suitable for applications that require cyclic loading and unloading [13,14].

In this context, it is important to note that the addition of short

* Corresponding author.
E-mail addresses: bgamboa@uma.es (C. Bermudo Gamboa), smartinb@uma.es (S. Martín-Béjar), trujillov@uma.es (J. Trujillo Vilches), lsevilla@uma.es (L. Sevilla Hurtado).

https://doi.org/10.1016/j.compscitech.2023.110205
Received 29 May 2023; Received in revised form 28 July 2023; Accepted 6 August 2023
Available online 12 August 2023

carbon fibres has an impact on the dimensional accuracy and macrogeometrical deviations of printed parts [15]. The viscosity and flow behaviour of the material affect its ability to be extruded, the accuracy of the printed part dimensions and its mechanical properties, being a disadvantage for the printing process itself [16].

On the other hand, several studies have investigated the effect of short carbon fibre reinforcement on the mechanical properties of PLA in additive manufacturing. For example, Gavali et al. [17] study how the addition of short carbon fibres (between 100 and 150 mm) improves the mechanical and thermomechanical properties of the composites, being a 15% the carbon fibre composition that shows the highest enhancement in tensile strength, flexural strength, impact strength, and hardness value. Shimamura et al. [18] discuss the fabrication of carbon nanofiller reinforced PLA and the measurement of its mechanical properties and heat resistivity. Vapor grown carbon fibre (VGCF) was used for reinforcement. The addition of VGCF to PLA increased the bending stiffness and heat deflection temperature but did not affect the bending strength up to 10% of VGCF. The imperfect adhesion between VGCF and matrix was seen, which resulted in pull-out of VGCFs over the fracture surfaces. This problem has been highlighted in this case study. The bad adhesion between the carbon fibres and the matrix creates gaps that work like stress concentrators and reduce the fatigue life of the printed parts. In the study of Lin et al. [19], the authors try to solve this problem by developing a sheet-like carbon fibre preform using short fibres to reinforce a geopolymer matrix. The resulting composite exhibits improved mechanical properties and non-catastrophic failure behaviour due to the fibre bridging and pulling-out the effect. In addition, Maqsood et al. [20], investigates the effect of adding continuous carbon fibre (CCF) to thermoplastic matrix to improve the mechanical properties of FFF parts. The study concludes that CCF reinforced PLA composite showed the highest tensile strength and Young's Modulus, while PLA-CCF specimens showed the largest mean flexural stress value. However, the improvement of the mechanical behaviour of PLA parts with short carbon fibres (1–3 mm) [15] as reinforcement is still an open discussion. Moreover, it must be highlighted that, most of the literature that analyses the mechanical properties of this material focuses mainly on the tensile strength. There is a lack of research involving other mechanical properties, such as fatigue behaviour [21–23]. To try to cover this gap, the present work analyses how the short carbon fibres directly affect the fatigue life of the printed parts, compared to the same samples printed only with PLA.

It is also important to consider the impact on dimensional accuracy and macrogeometrical deviations. These two characteristics have been proven to influence the fatigue life of the parts [23,24]. However, further research is needed to fully understand the interactions between mechanical properties, dimensional accuracy and geometric deviations when using this material (PLA + CF) in additive manufacturing applications. This case study covers the influence of the deviations commented with the fatigue life.

Fatigue is important for parts that are subjected to repetitive loading and unloading, such as those used in structural or mechanical applications [32,33]. This paper provides an analysis of how the printing parameters affect the fatigue behaviour of PLA reinforced with short carbon fibres in additive manufacturing and a comparison with PLA samples. The goal of this work is to provide a clear understanding of the printed parts behaviour under cyclic loading conditions using the rotational bending fatigue method, less studied, and to identify the key parameters that affect their fatigue resistance. Results show that the implementation of carbon fibres reduces 7% the fatigue life and the hypothesis is supported by fractographies, where the bad adhesion between PLA and the carbon fibres is presented. In addition, a parametric relationship is presented, relating the parameter that mainly influences the fatigue behaviour, the layer thickness, with the number of cycles.

2. Materials and methods

2.1. Sample material and 3D manufacturing

A blend of PLA with a 15% percentage of short CF (1–3 mm [15]), i3D, is chosen in a 1.75 mm filament form. A combination of the properties of both materials is obtained with this kind of filament. PLA is, in general, one of the most used materials in FFF, since it presents a particularly good printability. It requires low temperatures and is not greatly affected by the warping effect. This effect is the main cause of layer curvatures after their deposition and defects on the printed parts, due to a large temperature difference between layers. On the other hand, the carbon fibre is supposed to provide adhesion between layers, and a greater resistance to the final piece [25,26]. In general, this material combination is good option for parts that are subjected to demanding work conditions. However, one of the main objectives of this work is to determine if this behaviour is maintained for the fatigue behaviour of the parts.

The specimens are printed in a Raise 3D Pro2 printer. This printer presents a double extruder, with a maximum of 300 °C, a 0.01 mm of layer resolution and a working space of 280 × 305 × 300 mm. As for the printing parameters selected for this case study, is presented. The rest of the parameters remain constant. The selection of the printing parameters is based on previous studies [3,23] and the literature review [27,28]. In addition, the high printing speeds have been selected because of the importance of considering the impact of faster production of printed parts, bearing in mind that production times are always tending towards optimisation. Therefore, achieving 3D prints at higher speeds, without compromising the stability and characteristics of the part is considered an important objective.

The extruder nozzle is 0.8 mm wide to avoid material blocks with the carbon fibres, a very usual problem working with short fibre or particle composited materials. The bed temperature is set at 60 °C. The filling considered for this case study is linear, combined with 2 shells on the exterior of the printed parts. The printing direction of the samples is selected as horizontal, as it has been shown in other studies that the printed layers parallel to the load, shortens the fatigue life of the specimens [23,29]. Additionally, a comparison with samples printed only with PLA is conducted to better understand the behaviour of the short carbon fibre reinforcement.

The samples are designed with the SolidWorks software, from Dassault Systems [30], imported to the printer software, 3D Slicer Software IdeaMaker [31], as a .STL file. Four samples are printed for each printing parameter combination, having a total of 80 samples for this case study.

In addition, a series of control specimens have been manufactured only with PLA, to be able to analyse and compare the behaviour of the composite material (PLA + FC) with the polymeric material alone.

2.2. Dimensional control and macrogeometrical deviations

Dimension deviations are controlled with a digital Vernier calliper (STANDARD GAGE, model V-DIGIT CAL 200 mm–8 in THUMB), with a scale division of E = 0.01 mm and a two-contact micrometre for exterior measurements (MITUTOYO, range of use 0–25 mm), E = 0.01 mm. Fig. 1 shows the points there the diameter is controlled (1–9 manually with the micrometre and a-f automatically with the geometrical deviation measurement machine, for the B part). Each point is measured 4 times at different angles. This procedure is repeated for all the samples printed in order to make a correlation between the printing parameters and the dimensional deviations obtained.

As for the macrogeometrical deviations, the samples are controlled with a geometrical deviation measurement machine (ACCRETECH, model RONDCOM NEX) that presents a sensitivity of 0.01 μm. The specimens are fixed on the levelling as can be seen in Fig. 1 and the cero position is configured. The parameters controlled for this case study are the roundness (RON), the straightness (STR), the cylindricity (CYL) and

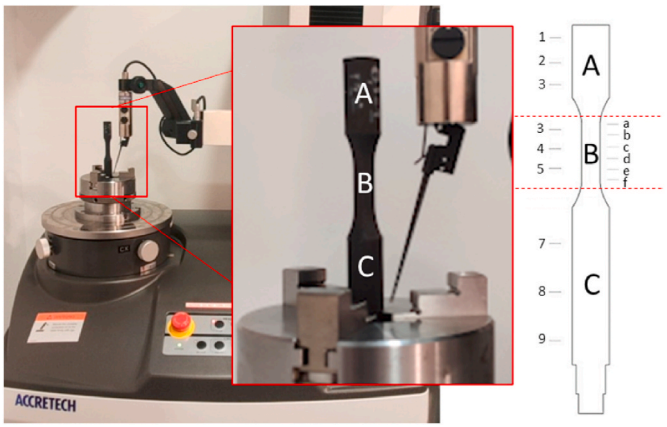

Fig. 1. Control-points (1–9, a-f) and sample zones (A–C).

the concentricity (CON).

The geometrical deviation measurement machine measures the values for RON and SRT and, with those values, CYL and CON are calculated.

To ensure repeatability, several measurements were carried out along the specimen. At three different highs or points for the zones A and C and at six points (a–f) for the calibrated zone B (Fig. 1). The roundness is expressed as the average result in the section measured. The straightness (STR) is controlled by 4 measurement lines that are taken at the 3 different areas, separated from each other by 90°. The measurements lines have a vertical length of 20 mm. From these data, the cylindricity (CYL) is calculated (see Fig. 1).

2.3. Sample geometry and fatigue test preparation

The ISO 1143:2010 standard [32] has been followed for the geometry of the samples, as it can be appreciated in Fig. 2. This standard has been selected due to the lack of specific standards for fatigue tests with polymeric samples manufactured by additive manufacturing. It is necessary to clarify that the left end of the samples (12 mm–Ø12 mm and 10 mm–Ø10 mm) is design for the fixation to the fatigue equipment, that can be seen in Fig. 3.

For a correct interpretation of the results and storage of the samples after testing, all the samples have been codified under a code that can rapidly identify the layer thickness (mm) [X_1], printing temperature (°C) [X_2] and printing speed (mm/s) [X_3], as for example, $X_1 + X_2 + X_3$, that

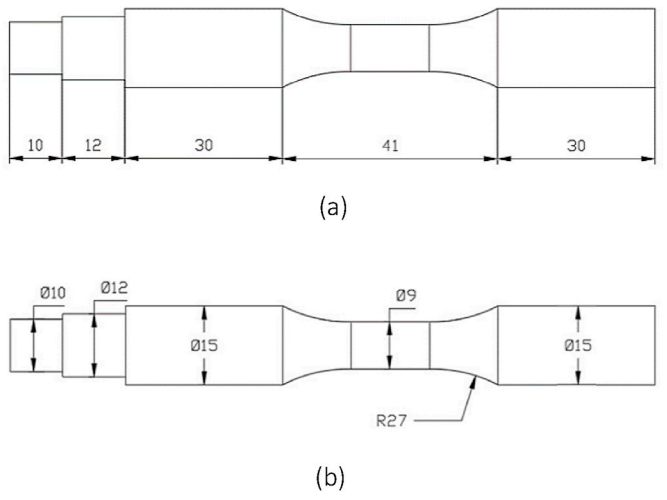

Fig. 2. Final sample dimensions. Longitudinal measurements (a) and diameters (b).

can be the 0.2 + 215 + 100 sample.

Once the deviations of the samples are controlled, according to their dimensions and geometry, the fatigue tests can be performed. The specimens are evaluated under a rotational bending fatigue equipment [33], shown before in Fig. 3. The equipment was designed and manufactured according to the ISO 1143:2010 standard [32], at the University of Malaga, by reusing the kinematic chain of an old parallel lathe out of service [24]. The equipment allows applying a single-point load on the extreme of the specimen (Fig. 3c and d).

Four different weighing configurations have been considered: 0.75, 0.9, 1 and 1.1 kgf. All of them set at a rotational speed of 1800 rev/min. After a threaded operation, the samples area attached at the machine through the clamp situated on the left and a tightening nut on the right, where the load is located (Fig. 3d).

Considering that the behaviour of the specimen is carried out at constant amplitude (Fatigue under Constant-Amplitude Loading), i.e. the load on the top of the specimen is the same as that on the bottom but one is tensile and the other compressive, the value of R is −1. In addition, considering the rotational speed 1800 rev/min, the frequency values would be 30 Hz.

When the samples break after undergoing the fatigue tests, they fall activating the stop sensor and the total cycles can be seen on the display. Then, the cycles and the distance from the breaking point to the load location are collected. To ensure the repeatability of the tests, the experiments has been carried out according to the ISO 12107:2012 standard [34] (95% confidence level and a 50% failure probability).

Considering the geometry of the specimen and the load applied, the equations that allows calculating the bending stress applied in the expected fracture section is:

$$S = \frac{32 \cdot F \cdot (L - x)}{\pi \cdot d^3} \quad (1)$$

where S corresponds to the stress at the fracture section (MPa), L to the distance between the load applied section and the fixed point (mm), x to the distance between the fixed point and the maximum stress point (mm), d to the calibrated area diameter (mm) and F to the Load applied (N) (Fig. 4).

3. Results and discussion

Having all the samples tested, the results are analysed to find out the influence of the carbon fibre reinforcement along with the different printing parameters studied.

3.1. Dimensional results

The first step is the dimensional analysis. As this case study deals with different printing variables, separated analysis have been carried out to understand the influence of each variable and have a general overview.

So, Fig. 5 shows a representation of the results obtained maintaining constant the printing speed or the temperature. The x-axis represents the measurement points where the samples have been controlled (Fig. 1). As it can be seen (Fig. 5a and c), the printing speed does not have a relevant influence except when a low temperature and a high speed are set. Fig. 5e presents only the values for 215 °C and 205 °C because at 100 mm/s, there is not enough time to the material to be deposited before causing a clog, as it can be seen in Fig. 6. Moreover, with a 100 mm/s printing speed, there is a difference between the temperatures implemented, being 215 °C the one that present less deviation from the original diameters (15 mm and 9 mm for the calibrated part) (Fig. 7e).

As for the temperature influence, again, the deviations obtained are similar with the different printing speed implemented (Fig. 5d and f), except when working with the highest temperature and speed from the selection (215 °C and 100 mm/s). In this case, the deviations obtained

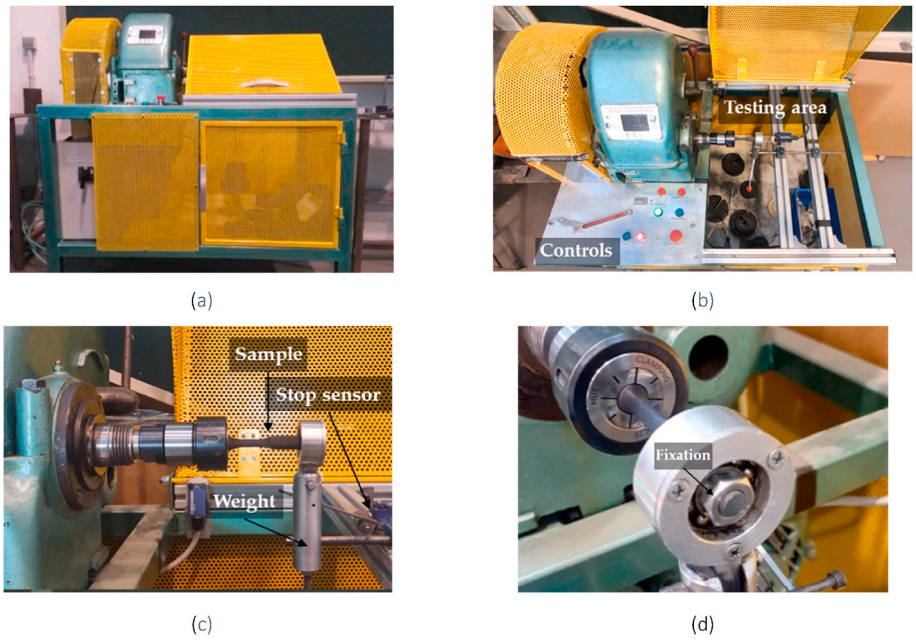

Fig. 3. Rotational bending fatigue equipment. Frontal and closed view (a), upper and open view (b) and sample undergoing the test (c).

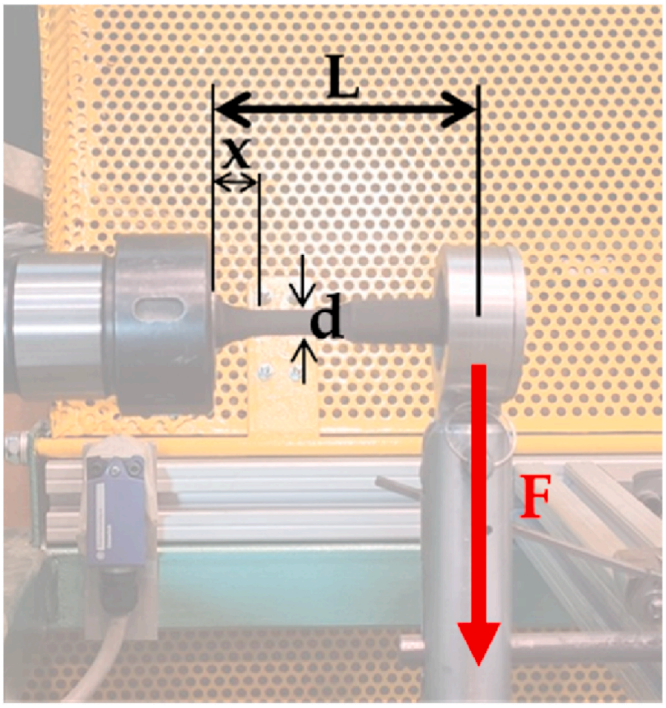

Fig. 4. Representation of the bending stress calculation.

are less.

This behaviour could be explained due to the contractions of the material when cooling down. As the extrusion temperature is high, the material extruded needs more time to cool down. Having a high printing speed, the heat from the next layer is shared with the layers that where already printed. So, the sample cools down in more time and the contractions are less. The hypothesis is that the next layers prevent the volumetric contractions of the previous layer, due to the printing temperature and the how fast the next layer is deposited. The standard deviations are presented with error bars. These deviations are in concordance with other studies [35–37].

Another comparison is made maintaining constant the printing speed and temperature, changing the layer thickness, as can be seen in Fig. 7. The printing temperature and speed have been set to the parameters that were considered optimal from the analysis in Fig. 5, that are 215 °C and 100 mm/s respectively. From the results, it can be state that 0.1 mm offers more deviations, a maximum of a 4.5% at the calibrated area and 7% at the non-calibrated parts.

It is clear that the manufacturing process alone makes it difficult to maintain a good dimensional control. The different layers or sections of the part are cooled in diverse ways and at different speeds, which means that the internal [38,39].

Additionally, a comparison with samples printed only with PLA has been taken into account, showing that the PLA samples present a more stable behaviour when the dimensional deviations are studied. So, is has to be stated that in this case study, the carbon fibre reinforcement does not improve the samples performance. PLA + CF is not a suitable alternative when the dimensional deviations of the printed parts have an important role.

3.2. Geometrical results

Fig. 8 present the results regarding the macrogeometrical deviations and the influence of the layer thickness, maintaining the same fixed parameters as in Figs. 7 and 215 °C and 100 mm/s. The results shown correspond with the maximum deviations obtained during measurements. It can be seen that there is not a general trend that can be stated. Overall, the samples with a 0.2 mm layer thickness less deviations. Moreover, it can be appreciated that, again, PLA + FC samples do not present a high improve behaviour when compared with PLA samples.

So, it can be stated that, in this case study, the improvement is not high enough to prioritize one material over the other. Furthermore, Fig. 8b shows a better behaviour of the PLA samples for the STR deviation.

Fig. 9 shows the results for the samples printed with the different temperatures and speed selected, maintaining the layer thickness at 0.2 mm, as is the one that offer a mayor stability on the calibrated part of the samples. For the roundness (Fig. 9a), the highest temperature offers lower deviations, and within the higher temperature, the lowest deviation is obtained with the lowest printing speed. However, it is not possible to stablish a clear tendency, as it can be appreciated that, at

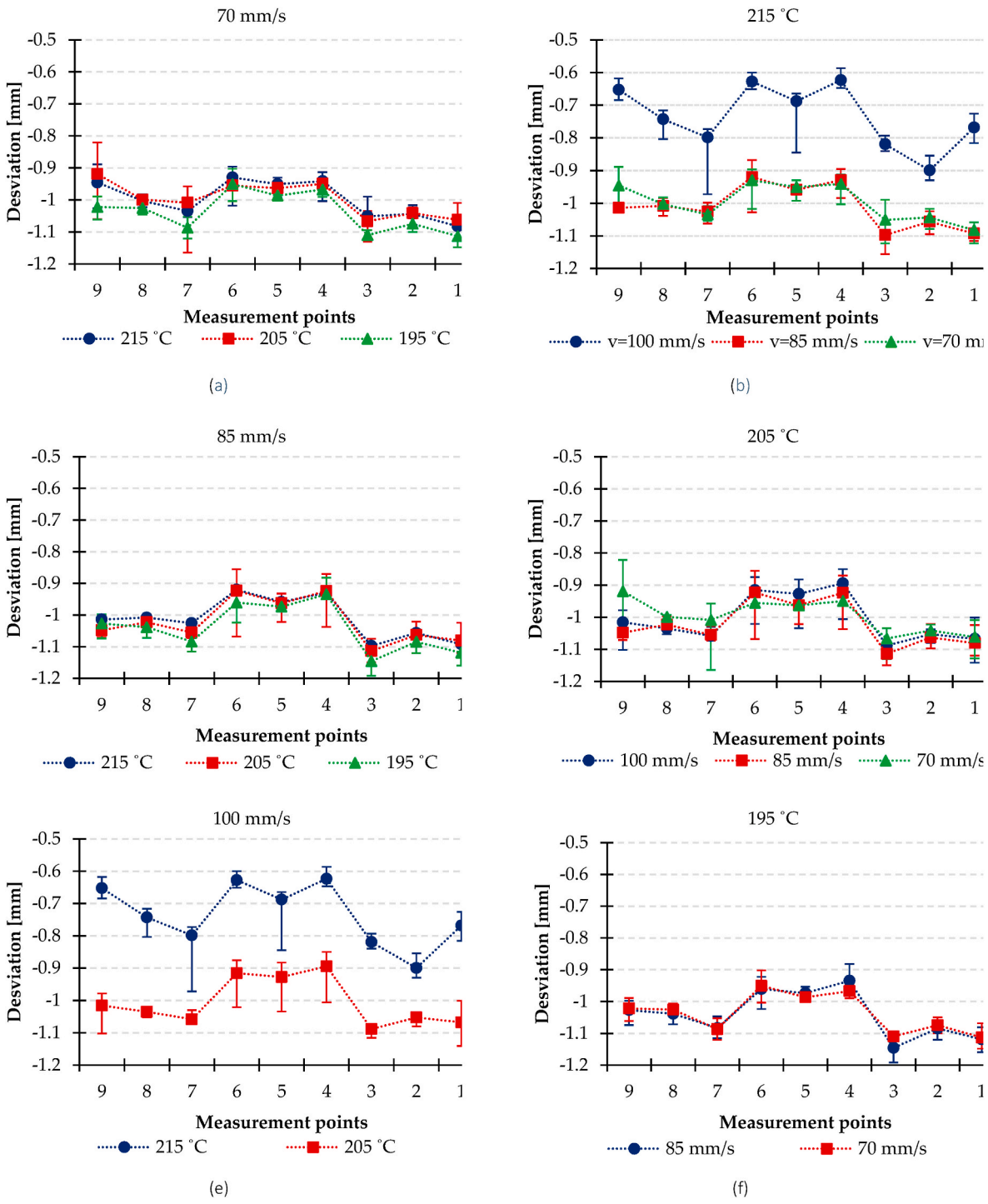

Fig. 5. Dimensional deviation results with a constant layer thickness of 0.2 mm and temperature and speed variations. Being 70 mm/s (a), 85 mm/s (c) and 100 mm/s (e) with temperature variation and 215 °C (b), 205 °C (d) and 195 °C (e) with speed variation.

205 °C, the highest deviations are obtained with the lowest speed.

The rest of the deviations studied present the same uneven behaviour (Fig. 9b–d). It is well known that quality control remains a major barrier to the wider application of AM in the manufacturing industry, with dimensional inaccuracy being a critical issue. It can be state that, in general, the deviations obtained with this kind of processes is high compared with other conventional processes like the machining process [40,41]. This case study corroborates the above, giving preference to the selection of PLA over PLA + CF.

3.3. Fatigue results

As for the fatigue results, different comparatives can be considered due to the number of tests performed and parameters analysed. According to the works referenced during the introduction, a selection of parameters is done for a first approximation of the analysis. One of the most influential parameters is the printing direction, which has been considered fixed as horizontal, due to the results obtained in previous studies, as commented in the introduction section [23,29]. Another crucial parameter for FFF in general is the layer thickness, which, has

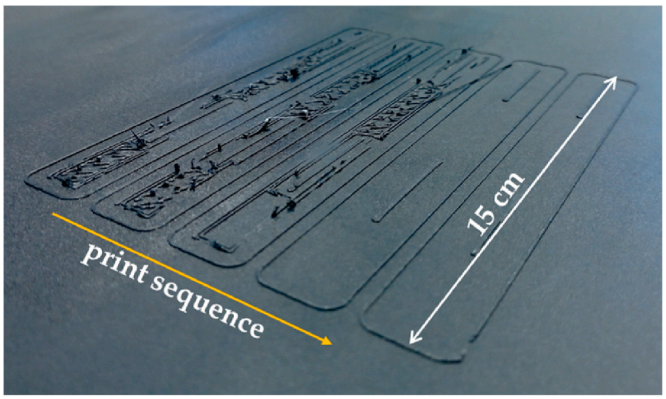

Fig. 6. Printing problems with the lowest temperature (195 °C) and high printing speeds (100 mm/s).

been set to 0.1, 0.2 and 0.3 mm, between the most common values [42,43]. However, for this first approximation to the fatigue behaviour, the layer thickness has been remained constant and the focus has been centred on the influence of the printing temperature and speed.

Fig. 10 presents the results obtained with the values selected for the temperature and the speed printing parameters. It needs to be highlighted that the breaking point has been measured for each sample. That explain the different stresses obtained for the same weight evaluated [24]. In general, all the samples break where the standard indicated but motivated by any of the different printing imperfection that are usual in FFF [44,45], there are some of the samples that can break before the indicated location. These printing imperfections can precipitate the crack and so, are considered as an anomalous behaviour. However, this anomalous behaviour is characteristic on fatigue studies, which present a certain uncertainty [24].

As the figures show (Fig. 10a and b), it can be seen that there is no great difference between the fatigue results obtained for a constant temperature and different speeds. There is one results that offers a lower stress, but this can be due to any of the possible defects that can appear

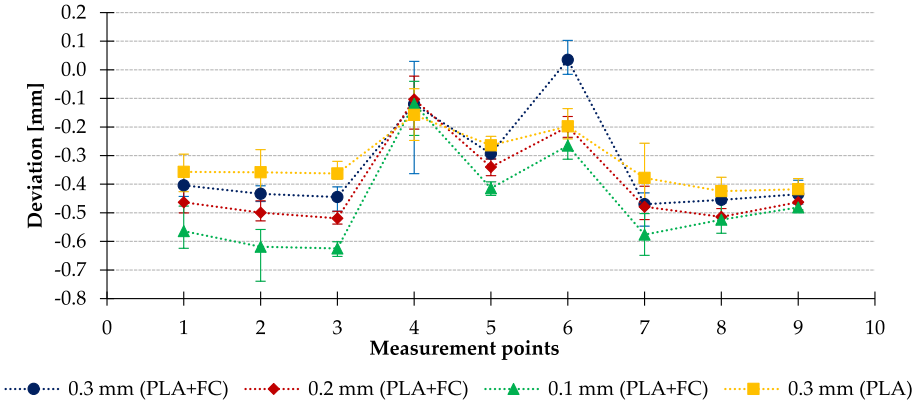

Fig. 7. Dimensional deviations for different layer thickness (mm), printing temperature and speed remaining constant at 215 °C and 100 mm/s, respectively.

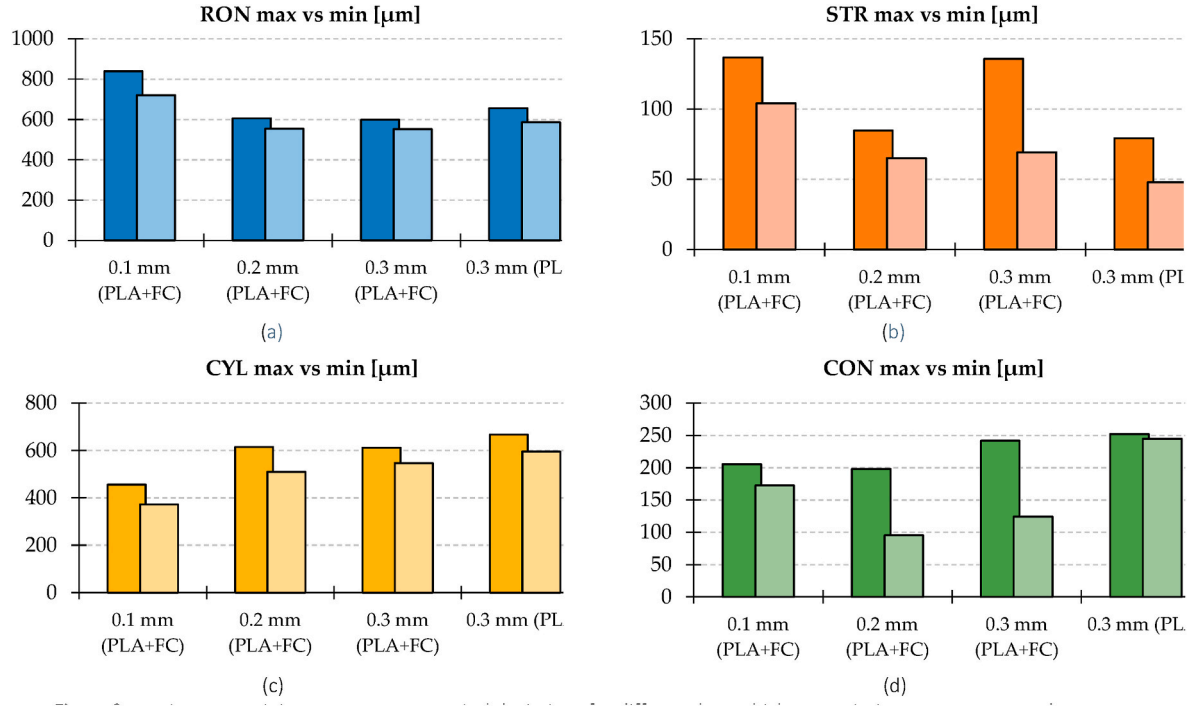

Fig. 8. Maximum vs minimum macrogeometrical deviations for different layer thickness, printing temperature and speed remaining constant at 215 °C and 100 mm/s respectively, being roundness (a), straightness (b), cylindricity (c) and concentricity (d).

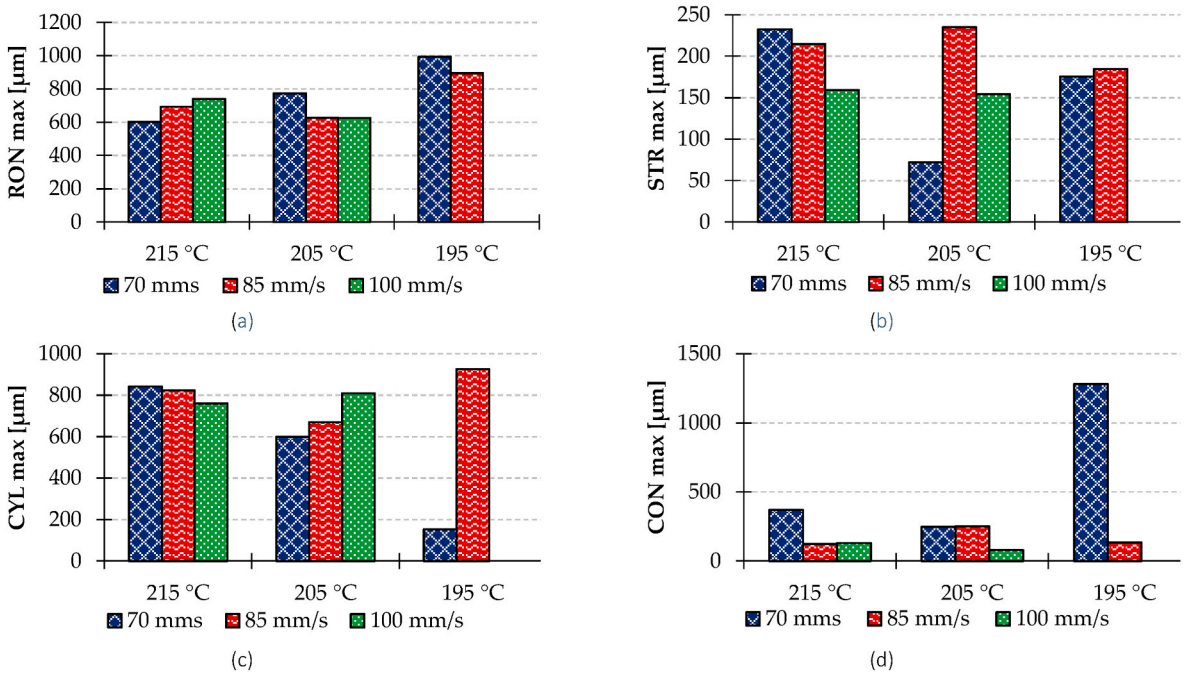

Fig. 9. Maximum macrogeometrical deviation for the different temperatures and speeds analysed, maintaining the layer thickness at 0.2 mm, being RON (a), STR (b) CYL mm/s (c) and CON.

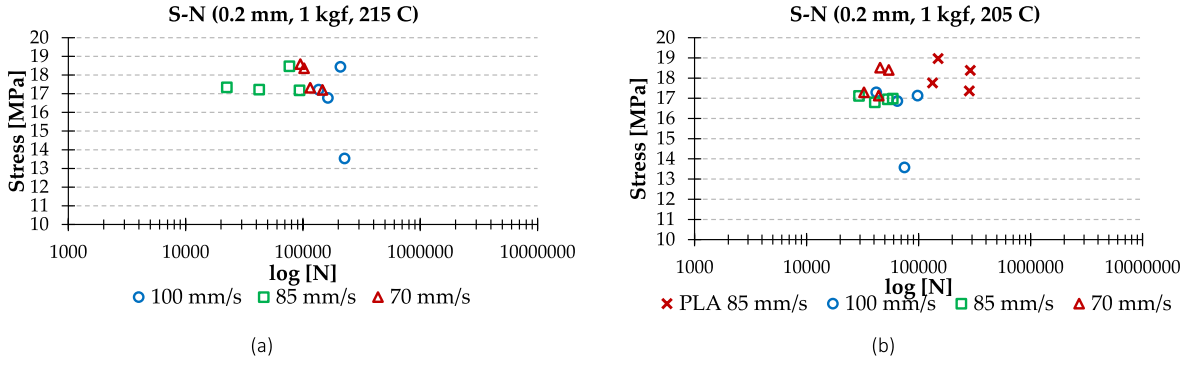

Fig. 10. Fatigue results according to printing temperature and speed variables, maintaining layer thickness and load constant. 215 °C and three speed considered (a) and 205 °C and three speed considered (b).

during the printing process. The fatigue tests usually present results with high dispersion, as commented.

Additionally, as it can be seen in Fig. 10, there is no set of results for the 195 °C printing temperature. Due to the low temperature, it is not possible to complete the printing of the sample with higher printing speed. It seems that there is not enough time for the material to be deposited. Moreover, the filament, due to the short carbon fibre reinforcement and low fluidization, tends to clog up the nozzle. Fig. 6 shows how the first layers were printed with the problems commented.

In general, it can be appreciated that a higher printing temperature slightly improves the fatigue behaviour as the results show a higher number of cycles before fail. However, it is not possible to identify a clear tendency, as the results show a better behaviour with the lowest and higher temperatures but equivalent results for the intermediate temperature.

In addition, there is a comparison between samples printed with PLA + FC and only with PLA in Fig. 10b. It can be appreciated how the reinforcement with short carbon fibres does not improve the behaviour of the samples under fatigue tests. The PLA samples show a better performance with more cycles under high stresses. This can be explained due to a bad adherence between the carbon fibres and the PLA matrix. The air gaps originated between these two elements create an easy crack propagation. So, there is not a continuity through all the material and the fatigue behaviour is worsen. However, it seems that for the greater thickness, the fatigue behaviour improves. This may be since the less thickness, the greater the number of layers and, therefore, a greater probability of crack initiation and growth.

This behaviour has a correlation with the images shown in Fig. 11. It can be appreciated how for layer thickness of 0.1 and 0.2 mm, the bad adhesion generates a separation between the exterior and interior shell (Fig. 11a and b). This behaviour seems to improve for 0.3 mm, where there is no sharp separation between layers (Fig. 11c). However, there are still areas where the adhesion between layers is not complete, as can be seen in the same image, marked with red arrows. For the PLA samples, it can be seen that the adhesion between layers is better. Fig. 11d shows an enlargement of the area, where a more homogeneous adhesion between layers can be seen. The exaggerated separation between layers that can be seen in PLA + FC specimens is due precisely to the lack of adhesion between the carbon fibres and the PLA matrix, which causes heterogeneous cooling and more exaggerated contractions and separations between layers.

Fig. 12 shows several SEM images obtained from PLA + CF samples

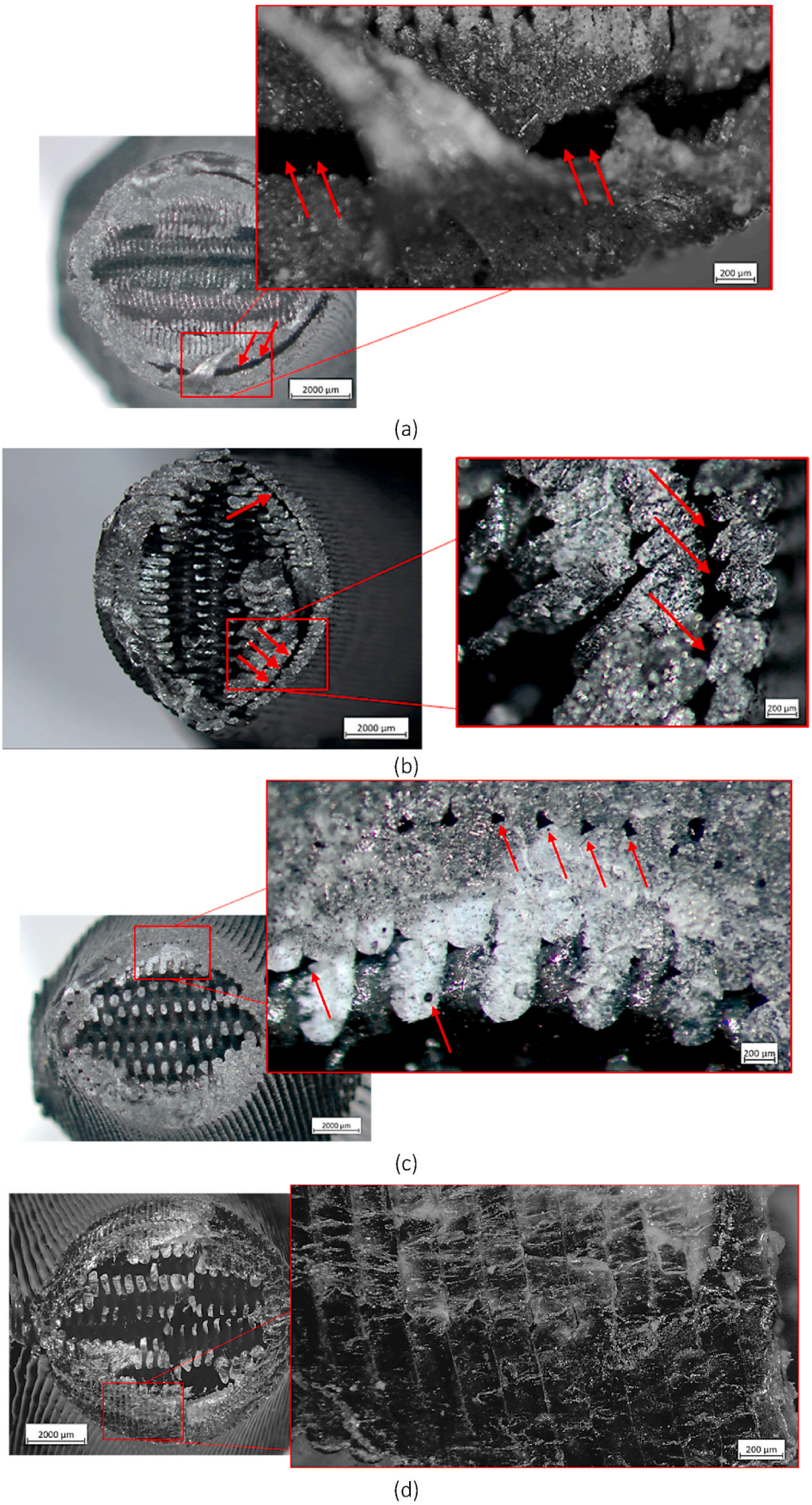

Fig. 11. Microscopies of different samples printed at 100 mm/s and 215 C, with different layer thickness: PLA + CF 0.1 mm (a) 0.2 mm (b) 0.3 mm (c) and 0.2 mm PLA (d).

and PLA samples. It can be clearly appreciated the lack of adherence between the short carbon fibres and the PLA matrix (Fig. 12a). This causes the fibre to peel off and creates these small cavities, which must be distinguished from the pores that can occur during the printing of the specimen. The gaps between the short fibres and the matrix work as stress concentrators, which shortens the fatigue life, as seen in the experimental results.

The porosity and cavities are not present in the PLA samples (Fig. 12b) and a better adhesion between layer can be seen.

As well, there is a direct relationship between the layer thickness and the stress. So, the higher the *e*, the higher the stress. This can be clearly appreciated in Fig. 13a–c for the lower loads tested, presenting a difference near a 40% on the stress sustained be (*e* 0.1 mm vs 0.3 mm). However, it can be highlighted that, for the higher load tested (Fig. 13d), the improvement on the stress endured according to *e* can still be appreciated but the difference between layer thickness tends to even out, presenting a 16% difference between *e* 0.1 mm and 0.3 mm.

Additionally, a clear difference according to the layer thickness is presented in Fig. 13a, for the lowest load tested. For 0.9 kgf (Fig. 13b) the 0.2 mm layer thickness samples tend to follow the 0.3 mm samples and, for 1 kgf (Fig. 13c) the 0.1 mm layer thickness samples tend to have a similar behaviour as the 0.2 mm samples. It can be appreciated that the higher the layer thickness, the higher the stress values are compared to the ones obtained for the lower layer thicknesses. This is because at higher layer thicknesses, the specimen breaks closer to the maximum stress near the radius of curvature. However, at lower layer thicknesses, the stress is smaller because the break is not in the expected area due to the number of layers.

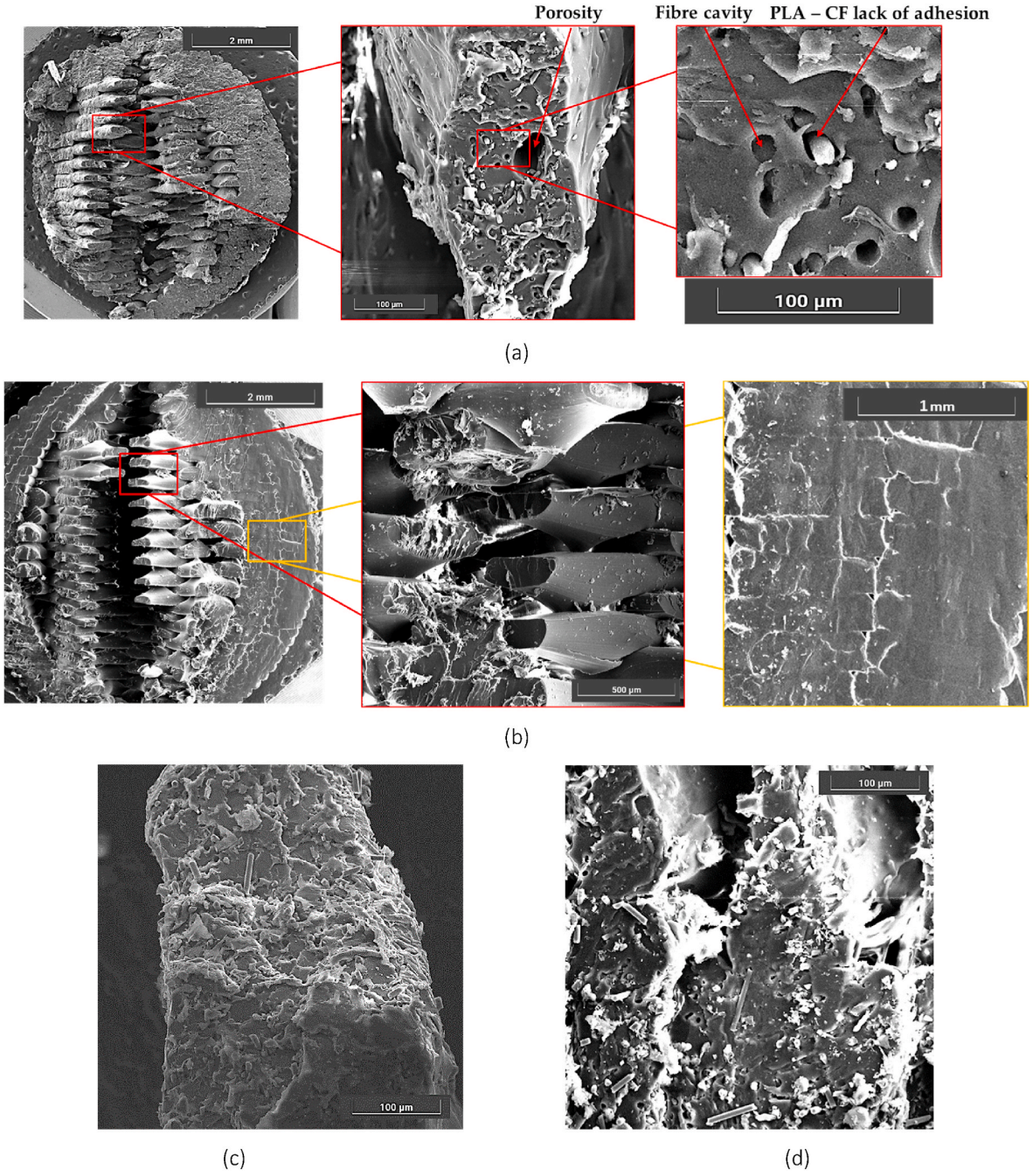

Fig. 12. SEM images of different samples printed at 100 mm/s and 215 C, with different layer thickness: PLA + CF 0.2 mm (a) PLA 0.2 mm (b) 0.3 (c) and carbon fibres detail (c and d).

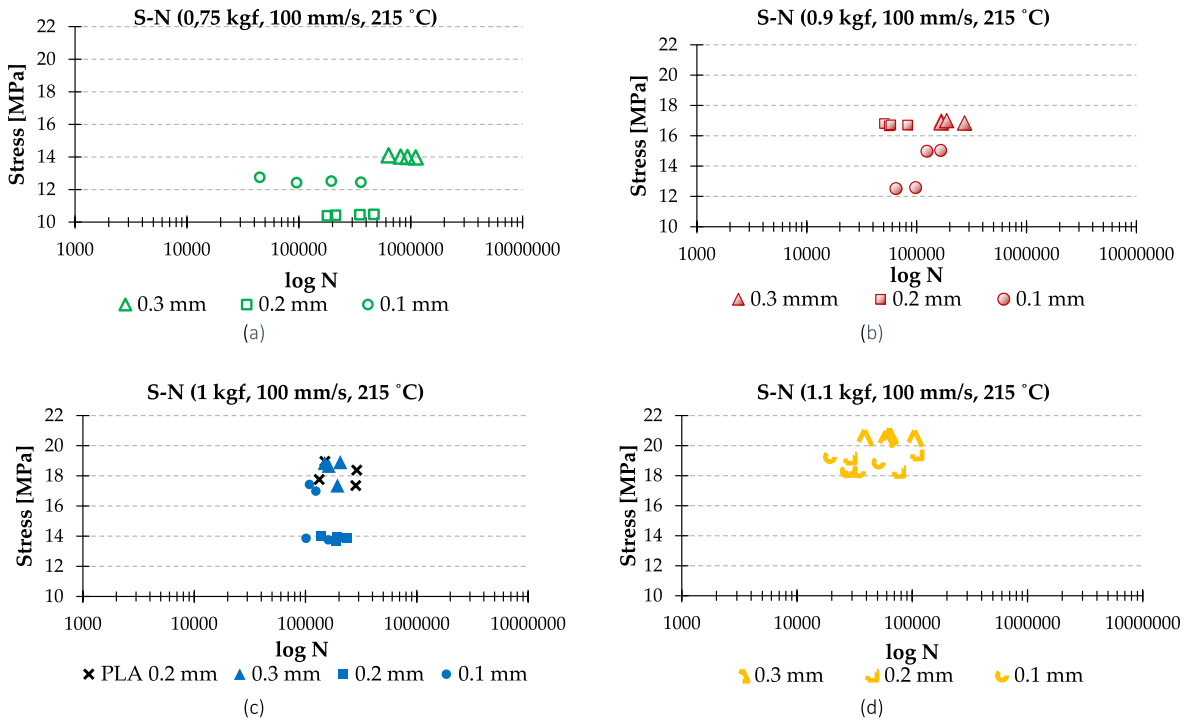

Fig. 13. Fatigue results according to the layer thickness and the load. All layer thickness selected and 0.75 kgf (a), 0.9 kgf (b), 1 kgf (c) and 1.1 kgf (d).

As commented before, the layers are considered as stress concentrators because of the discontinuity they cause on the surface of the printed part. Therefore, the greater the number of layers, the more likely will be to break in an area other than the expected, where the stress is lower. Although the applied force is the same, the values are different because the stress value has been adjusted to the real value of breakage, not the theoretical value.

So, it can be determined that the layer thickness can be decisive when working with lower loads. Nevertheless, when the load tends to increase, a thicker layer does not provide a substantial improvement to the parts. However, from a security point of view, it will be recommended to design the parts with a thicker layer (Fig. 13d).

Analysing the results according to the printing parameters and the different loads implemented, an equation that relates the fatigue life with the load and the printing parameters analysed for this case study can be suggested. The results obtained are in agreement with fatigue results obtained in different studies, to consult Fig. s10 in Ref. [46], Figs. s7 and 8 in Ref. [47] or Fig. s8 in Ref. [48].

The Basquin's equation, which relates S–N, is obtained for each printing parameter combination (Eq. (2)).

$$S = C \cdot N^{\alpha} \tag{2}$$

Being C and α constant (see Table 1). Fig. 14 shows how this type of potential equation fits the experimental data using a linear regression (log-log). Table 2 shows the results for these constants according to ISO 12107:2012 [34]. The parametric relationship presents a reasonable fit (R^2), considering the usual dispersion of the fatigue results.

It can be seen that for smaller layer thickness it is more likely for the sample to break in another point, represented by the results dispersion. This behaviour is less evident at lower stress values. Moreover, the behaviour of R^2 gets worse when lowering the layer thickness. This is because at 0.1 mm is more difficult to adjust the behaviour of the material, due to the same dispersion presented on the results obtained. It can be considered that the union between layers, which lack of continuity or adherence, facilitates the growth of the crack.

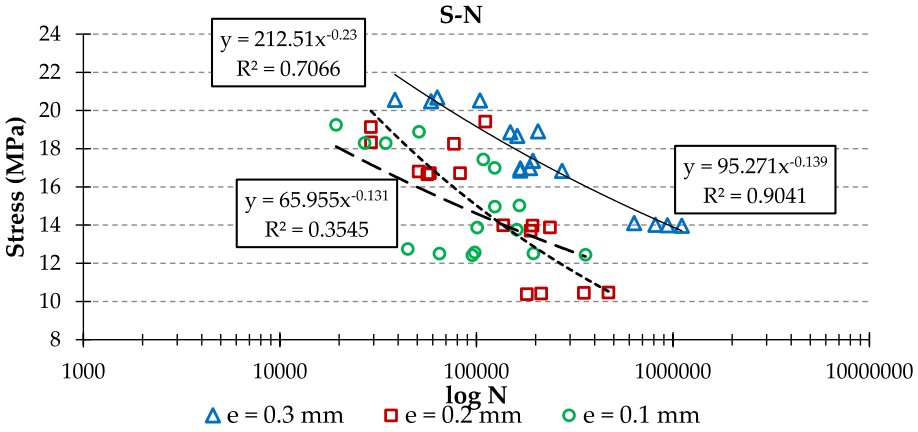

Fig. 14. Fatigue results evolution according to the different layer thickness (*e*) implemented, temperature, speed, filling and nozzle remaining constant (215 °C, 100 mm/s, 50% and 0.8 mm).

Table 1
Printing parameters.

PLA + FC (black)	*v* [mm/s]	70			85			100				
	T [°C]	195	205	215	195	205	215	195	205	215		
	e [mm]	0.2								0.1	0.2	0.3
	Filling [%]	50										
PLA (red)	*v* [mm/s]	100										
	T [°C]	215										
	e [mm]	0.2										
	Filling [%]	50										

Table 2
S–N potential equation results.

e [mm]	*T* [°C]	*v* [mm/s]	%	Nozzle [mm]	C	α	R^2
0.1	215	100	50	0.8	65.955	−0.131	0.3545
0.2					212.51	−0.23	0.7066
0.3					95.271	−0.139	0.9041

4. Conclusions

In this case study, the behaviour of samples printed with short carbon fibre reinforced PLA and different printing temperatures, speeds, and layer thicknesses has been analysed. The results help to understand the influence of the printing parameters on the fatigue behaviour and on the dimensional and macrogeometrical deviations of the samples. Moreover, the case study is focus in high printing speeds, compared with the references cited along the text. The main conclusions are:

- The analysis indicates that the layer thickness has a significant impact on the dimensional deviations, being the layer thickness of 0.2 mm the one that offers less deviations in general (3% at the calibrated area), with 0.1 mm offering the higer deviations (4.5% at the calibrated part), among the tested values.
- The printing speed does not have a considerable influence on the dimensional accuracy except when a low temperature (195 °C) and high speed are set (100 mm/s). On the contrary, the extrusion temperature has a greater influence on dimensional accuracy, with higher temperatures resulting in less deviation from the original diameters. There is a 20% difference for the RON deviation when working at 215 °C comparing 70–100 mm/s versus a 99% difference with 70 mms and 215-195 °C. Results show that at the higher speed, the results are stable, having a higher fluctuation with 70 and 85 mm/s. However, at high speed, a high printing temperature is also needed to avoid clogs.
- The printing temperature slightly improves the fatigue behaviour, but the short carbon fibre reinforcement does not improve the behaviour of the samples under fatigue tests. There is no significant difference between the fatigue results obtained for a constant temperature and different speeds.
- Samples printed with PLA only exhibit a more stable behaviour (less dispersion and diameter deviation) when dimensional deviations are studied and show a better performance with more cycles under high stresses in fatigue tests, compared to samples printed with PLA + FC (6% stress improvement and over a 60% in the number of cycles before sample fail). This can be explained due to the air gaps originated between the short carbon fibres and the PLA matrix, due to a bad adherence within these two elements, acting like stress concentrators.
- An equation that can predict the fatigue life of the PLA + FC material based on the load and printing parameters analysed in the case study has been developed. The Basquin's equation has been used to obtain the equation and the constant values of C and α were determined for each printing parameter combination according to ISO 12107:2012. The experimental data fits this potential equation well, and the results show a reasonable fit, with $R^2 = 0.89$ for $e = 0.3$ mm and $R^2 = 0.70$ for $e = 0.2$ mm). Therefore, the equation proposed in this study can be useful in predicting the fatigue life of materials under specific printing parameters and loads. R^2 for the lowest thickness layer tested (0.1 mm) does not show a good fit. However, it is not recommended to work with that *e* because according to the results obtained in this case study.
- It has been estimated that the fatigue behaviour improves with greater layer thickness. This may be since the crack initiates and propagate between layers and the smaller the layer thickness, the greater the number of layers the samples present.
- According to the results obtained, the selection of PLA + CF over PLA is not recommended.

Author contributions

Conceptualization, CBG and SM.; methodology SM; data interpretation CBG and SM; writing—original draft preparation, CBG.; writing—review and editing, CBG and SM; supervision, FJT and LS.; All authors have read and agreed to the published version of the manuscript.

Declaration of competing interest

The authors declare that they have no known competing financial interests or personal relationships that could have appeared to influence the work reported in this paper

Data availability

Data will be made available on request.

Acknowledgments

The authors thank the University of Malaga-Andalucia Tech Campus of International Excellence.

References

[1] F. Lederle, F. Meyer, G.P. Brunotte, C. Kaldun, E.G. Hübner, Improved mechanical properties of 3D-printed parts by fused deposition modeling processed under the exclusion of oxygen, Progress Addit. Manuf. 1 (2016) 3–7, https://doi.org/10.1007/S40964-016-0010-Y.
[2] B. Gao, Q. Yang, X. Zhao, G. Jin, Y. Ma, F. Xu, 4D bioprinting for biomedical applications, Trends Biotechnol. 34 (2016) 746–756, https://doi.org/10.1016/j.tibtech.2016.03.004.
[3] C. Bermudo Gamboa, S. Martín Béjar, F.J. Trujillo Vilches, L. Sevilla Hurtado, Geometrical analysis in material extrusion process with polylactic acid (PLA)+ carbon fiber, Rapid Prototyp. J. 29 (2022) 21–39, https://doi.org/10.1108/RPJ-09-2022-0294/FULL/PDF.
[4] K. Rajan, M. Samykano, K. Kadirgama, W.S.W. Harun, M.M. Rahman, Fused deposition modeling: process, materials, parameters, properties, and applications, Int. J. Adv. Des. Manuf. Technol. 120 (2022) 1531–1570, https://doi.org/10.1007/S00170-022-08860-7.
[5] F.M. Mwema, E.T. Akinlabi, in: F.M. Mwema, E.T. Akinlabi (Eds.), Basics of fused deposition modelling (FDM), Fused Deposition Modeling: Strategies for Quality Enhancement, Springer International Publishing, Cham, 2020, pp. 1–15, 978-3-030-48259-6.

[6] S. Rouf, A. Malik, N. Singh, A. Raina, N. Naveed, M.I.H. Siddiqui, M.I.U. Haq, Additive manufacturing technologies: industrial and medical applications, Sustain. Oper. Comput. 3 (2022) 258–274, https://doi.org/10.1016/j.susoc.2022.05.001.
[7] R.B. Kristiawan, F. Imaduddin, D. Ariawan, Ubaidillah, Z. Arifin, A review on the fused deposition modeling (FDM) 3D printing: filament processing, materials, and printing parameters, Open Eng. 11 (2021) 639–649, https://doi.org/10.1515/ENG-2021-0063/ASSET/GRAPHIC/J_ENG-2021-0063_FIG_003.JPG.
[8] D.D. Hernandez, Factors affecting dimensional precision of consumer 3D printing, Int. J. Aviat., Aeronaut., Aerosp. 2 (2015), https://doi.org/10.15394/IJAAA.2015.1085.
[9] A. Mohanty, K.S. Nag, D.K. Bagal, A. Barua, S. Jeet, S.S. Mahapatra, H. Cherkia, Parametric optimization of parameters affecting dimension precision of FDM printed part using hybrid Taguchi-MARCOS-nature inspired heuristic optimization technique, Mater. Today Proc. 50 (2022) 893–903, https://doi.org/10.1016/J.MATPR.2021.06.216.
[10] P. Ferretti, C. Leon-Cardenas, G.M. Santi, M. Sali, E. Ciotti, L. Frizziero, G. Donnici, A. Liverani, Relationship between FDM 3D printing parameters study: parameter optimization for lower defects, Polymers (Basel) 13 (2021), https://doi.org/10.3390/polym13132190.
[11] M. Khorasani, A. Ghasemi, B. Rolfe, I. Gibson, Additive manufacturing a powerful Tool for the aerospace industry, Rapid Prototyp. J. 28 (2022) 87–100, https://doi.org/10.1108/RPJ-01-2021-0009.
[12] R.A. Ilyas, S.M. Sapuan, M.M. Harussani, M.Y.A.Y. Hakimi, M.Z.M. Haziq, M.S. N. Atikah, M.R.M. Asyraf, M.R. Ishak, M.R. Razman, N.M. Nurazzi, et al., Polylactic acid (PLA) biocomposite: processing, additive manufacturing and advanced applications, Polymers (Basel) 13 (2021), https://doi.org/10.3390/polym13081326.
[13] P. Wang, B. Zou, S. Ding, C. Huang, Z. Shi, Y. Ma, P. Yao, Preparation of short CF/GF reinforced PEEK composite filaments and their comprehensive properties evaluation for FDM-3D printing, Compos. B Eng. 198 (2020), 108175, https://doi.org/10.1016/J.COMPOSITESB.2020.108175.
[14] S. Khan, K. Joshi, S. Deshmukh, A comprehensive review on effect of printing parameters on mechanical properties of FDM printed parts, Mater. Today Proc. 50 (2022) 2119–2127, https://doi.org/10.1016/J.MATPR.2021.09.433.
[15] N. Krajangsawasdi, L.G. Blok, I. Hamerton, M.L. Longana, B.K.S. Woods, D. S. Ivanov, Fused deposition modelling of fibre reinforced polymer composites: a parametric review, J. Compos. Sci. 5 (2021), https://doi.org/10.3390/jcs5010029.
[16] F.D.C. Siacor, Q. Chen, J.Y. Zhao, L. Han, A.D. Valino, E.B. Taboada, E.B. Caldona, R.C. Advincula, On the additive manufacturing (3D printing) of viscoelastic materials and flow behavior: from composites to food manufacturing, Addit. Manuf. 45 (2021), 102043, https://doi.org/10.1016/J.ADDMA.2021.102043.
[17] V.C. Gavali, P.R. Kubade, H.B. Kulkarni, Mechanical and Thermo-mechanical properties of carbon fiber reinforced thermoplastic composite fabricated using fused deposition modeling method, Mater. Today Proc. 22 (2020) 1786–1795, https://doi.org/10.1016/J.MATPR.2020.03.012.
[18] Y. Shimamura, A. Yamamoku, K. Tohgo, S. Tasaka, H. Araki, Mechanical properties of carbon nanofiber reinforced polylactic acid, Key Eng. Mater. 345–346 (2007) 1225–1228, https://doi.org/10.4028/WWW.SCIENTIFIC.NET/KEM.345-346.1225.
[19] T. Lin, D. Jia, P. He, M. Wang, D. Liang, Effects of fiber length on mechanical properties and fracture behavior of short carbon fiber reinforced geopolymer matrix composites, Mater. Sci. Eng., A 497 (2008) 181–185, https://doi.org/10.1016/J.MSEA.2008.06.040.
[20] N. Maqsood, M. Rimašauskas, Characterization of carbon fiber reinforced PLA composites manufactured by fused deposition modeling, Compos. Part C: Open Access 4 (2021), 100112, https://doi.org/10.1016/J.JCOMC.2021.100112.
[21] S. Wickramasinghe, T. Do, P. Tran, FDM-based 3D printing of polymer and associated composite: a review on mechanical properties, defects and Treatments, Polymers (Basel) 12 (2020) 1–42, https://doi.org/10.3390/POLYM12071529.
[22] G. Gomez-Gras, R. Jerez-Mesa, J.A. Travieso-Rodriguez, J. Lluma-Fuentes, Fatigue performance of fused filament fabrication PLA specimens, Mater. Des. 140 (2018) 278–285, https://doi.org/10.1016/J.MATDES.2017.11.072.
[23] A.G. Montesinos, C.B. Gamboa, S.M. Bejar, L.S. Hurtado, Influence of Layer Thickness on Fatigue Life of PLA + Carbon Fiber Specimens by Additive Manufacturing, 2023, pp. 401–412, https://doi.org/10.1007/978-3-031-20325-1_31.
[24] S.M. Béjar, F.J.T. Vilches, C.B. Gamboa, L.S. Hurtado, Fatigue behavior parametric analysis of dry machined Uns A97075 aluminum alloy, Metals (Basel) 10 (2020), https://doi.org/10.3390/met10050631.
[25] S.S. Yao, F.L. Jin, K.Y. Rhee, D. Hui, S.J. Park, Recent advances in carbon-fiber-reinforced thermoplastic composites: a review, Compos. B Eng. 142 (2018) 241–250, https://doi.org/10.1016/J.COMPOSITESB.2017.12.007.
[26] G. Liao, Z. Li, Y. Cheng, D. Xu, D. Zhu, S. Jiang, J. Guo, X. Chen, G. Xu, Y. Zhu, Properties of oriented carbon fiber/polyamide 12 composite parts fabricated by fused deposition modeling, Mater. Des. 139 (2018) 283–292, https://doi.org/10.1016/J.MATDES.2017.11.027.
[27] N. Yodo, A. Dey, in: H.K. Dave, J.P. Davim (Eds.), Multi-Objective Optimization for FDM Process Parameters with Evolutionary Algorithms BT - Fused Deposition Modeling Based 3D Printing, Springer International Publishing, Cham, 2021, ISBN 978-3-030-68024-4, pp. 419–444.
[28] D. Rahmatabadi, A. Aminzadeh, M. Aberoumand, M. Moradi, in: H.K. Dave, J. P. Davim (Eds.), Mechanical Characterization of Fused Deposition Modeling (FDM) 3D Printed Parts BT - Fused Deposition Modeling Based 3D Printing, Springer International Publishing, Cham, 2021, ISBN 978-3-030-68024-4, pp. 131–150.
[29] G. Gomez-Gras, R. Jerez-Mesa, J.A. Travieso-Rodriguez, J. Lluma-Fuentes, Fatigue performance of fused filament fabrication PLA specimens, Mater. Des. 140 (2018) 278–285, https://doi.org/10.1016/J.MATDES.2017.11.072.
[30] SOLIDWORKS, Available online, https://www.solidworks.com/es (accessed on 13 March 2023).
[31] Powerful 3D Slicer Software, IdeaMaker by Raise3D, Available online, https://www.raise3d.com/ideamaker/ (accessed on 13 March 2023).
[32] ISO ISO 1143, Standard. Metallic Materials — Rotating Bar Bending Fatigue Testing vol. 2010, ISO, 2010.
[33] F.J. Trujillo, S. Martín-Béjar, C. Bermudo, L. Sevilla, Fatigue test bench manufacturing by reusing a parallel lathe, in: Proceedings of the Advances in Transdisciplinary Engineering, vol. 8, IOS Press BV, 2018, pp. 15–20.
[34] ISO - ISO 12107, Metallic materials — fatigue testing — statistical planning and analysis of Data Available online. https://www.iso.org/standard/50242.html, 2012 (accessed on 23 November 2022).
[35] G. Gómez-Gras, M.A. Pérez, J. Fábregas-Moreno, G. Reyes-Pozo, Experimental study on the accuracy and surface quality of printed versus machined holes in PEI Ultem 9085 FDM specimens, Rapid Prototyp. J. 27 (2021) 1–12, https://doi.org/10.1108/RPJ-12-2019-0306/FULL/PDF.
[36] I. Buj-Corral, E.E. Zayas-Figueras, Comparative study about dimensional accuracy and form errors of FFF printed spur gears using PLA and nylon, Polym. Test. 117 (2023), 107862, https://doi.org/10.1016/J.POLYMERTESTING.2022.107862.
[37] E.E. Zayas-Figueras, I. Buj-Corral, Comparative study about dimensional accuracy and surface finish of constant-breadth cams manufactured by FFF and CNC milling, Micromachines 14 (2023) 377, https://doi.org/10.3390/MI14020377.
[38] B. Redwood, F. Schöffer, B. Garret, The 3D Printing Handbook, 3D Hubs, 2017, p. 304.
[39] Q. Sun, Z. Shan, L. Zhan, S. Wang, X. Liu, Z. Li, S. Wu, Warp deformation model of polyetheretherketone composites reinforced with carbon fibers in additive manufacturing, Mater. Res. Express 8 (2021), 125305, https://doi.org/10.1088/2053-1591/ABEEC8.
[40] S. Chowdhury, S. Anand, Artificial Neural Network Based Geometric Compensation for Thermal Deformation in Additive Manufacturing Processes, vol. 3, 2016.
[41] L. Cheng, A. Wang, F. Tsung, A Prediction and Compensation Scheme for In-Plane Shape Deviation of Additive Manufacturing with Information on Process Parameters, vol. 50, 2018, pp. 394–406, https://doi.org/10.1080/24725854.2017.1402224.
[42] J.M. Chacón, M.A. Caminero, E. García-Plaza, P.J. Núñez, Additive manufacturing of PLA structures using fused deposition modelling: effect of process parameters on mechanical properties and their optimal selection, Mater. Des. 124 (2017) 143–157, https://doi.org/10.1016/j.matdes.2017.03.065.
[43] R. Jerez-Mesa, J.A. Travieso-Rodriguez, J. Llumà-Fuentes, G. Gomez-Gras, D. Puig, Fatigue lifespan study of PLA parts obtained by additive manufacturing, Procedia Manuf. 13 (2017) 872–879, https://doi.org/10.1016/J.PROMFG.2017.09.146.
[44] M. Baechle-Clayton, E. Loos, M. Taheri, H. Taheri, Failures and flaws in fused deposition modeling (FDM) additively manufactured polymers and composites, J. Compos. Sci. 6 (2022) 202, https://doi.org/10.3390/JCS6070202.
[45] P.K. Penumakala, J. Santo, A. Thomas, A critical review on the fused deposition modeling of thermoplastic polymer composites, Compos. B Eng. 201 (2020), 108336, https://doi.org/10.1016/J.COMPOSITESB.2020.108336.
[46] H.R. Vanaei, M. Shirinbayan, S. Vanaei, J. Fitoussi, S. Khelladi, A. Tcharkhtchi, Multi-scale damage analysis and fatigue behavior of PLA manufactured by fused deposition modeling (FDM), Rapid Prototyp. J. 27 (2021) 371–378, https://doi.org/10.1108/RPJ-11-2019-0300/FULL/PDF.
[47] M.S.A. Parast, A. Bagheri, A. Kami, M. Azadi, V. Asghari, Bending fatigue behavior of fused filament fabrication 3D-printed ABS and PLA joints with rotary friction welding, Progress Addit. Manuf. 7 (2022) 1345–1361, https://doi.org/10.1007/S40964-022-00307-5/FIGURES/19.
[48] P. Kiani, M. Sedighi, M. Kasaeian-Naeini, A.H. Jabbari, High cycle fatigue behavior and thermal properties of PLA/PCL blends produced by fused deposition modeling, J. Polym. Res. 30 (2023) 264, https://doi.org/10.1007/s10965-023-03651-4.